REMOTE SENS. ENVIRON. 41:1–17 (1992)

Estimating Structural Attributes of Douglas-Fir/ Western Hemlock Forest Stands from Landsat and SPOT Imagery

Warren B. Cohen and Thomas A. Spies

USDA, Forest Service, Pacific Northwest Research Station, Forestry Sciences Laboratory, Corvallis, Oregon

To help determine the utility of satellite data for analysis and inventory of Douglas-fir/western hemlock forests west of the Cascade Mountains crest in Oregon and Washington, USA, we evaluate relationships between spectral and texture variables derived from SPOT HRV 10 m panchromatic and LANDSAT TM 30 m multispectral data and 16 forest stand structural attributes. Texture of the HRV data was strongly related to many of the stand attributes evaluated, whereas TM texture was weakly related to all attributes. Wetness, a feature of the TM Tasseled Cap, was the spectral variable most highly correlated to all stand attributes. Wetness appears to respond to the degree of maturity in a forest stand. One of the primary reasons HRV texture and TM wetness exhibited strong relationships with stand attributes is their relative insensitivity to topographically induced illumination angle. Although TM texture also was insensitive to topography, the spatial resolution of TM data is too coarse to detect the spatial variability within the forest stands evaluated. Regression models used to estimate values for the stand attributes from the satellite data indicate that both TM and HRV imagery should yield equally accurate estimates of forest age class and stand structure. Of all stand attributes evaluated, the standard deviation of tree sizes, mean size and density of trees in the upper canopy layers, a structural complexity index, and stand age can be most reliably estimated using the satellite data.

INTRODUCTION

The extent and condition of old-growth conifer forest remaining in the western United States and Canada is of great interest to a number of land management agencies, forest industries, and public groups. This interest has created an urgent need to characterize old growth, distinguish it from younger stands, and to identify the location of individual old-growth patches across the landscape. As a result, there are numerous concurrent studies designed to accomplish these objectives [see *Focus on Old-Growth Forests of Northwestern North America, Northwest Environ. J.* 6(2), 1990].

Given the immediate need for information, and the large areal extent of the region over which old-growth forests can be found, satellite imagery is being used as a primary source of data in studies focusing on inventory and mapping (Woodcock et al., 1990; Niemann et al., 1991; Teply and Green, 1991; Wilderness Society, 1991). A number of different image analysis techniques are

Address correspondence to Warren B. Cohen, USDA, Forest Service, Pacific Northwest Research Station, Forestry Sciences Lab., 3200 SW Jefferson Way, Corvallis, OR 97331.

Received 15 July 1991; revised 18 January 1992.

0034-4257/92/$0.00
Published 1992 by Elsevier Science Publishing Co. Inc.
655 Avenue of the Americas, New York, NY 10010

being used in these studies to map forest conditions. These include photointerpretation of the satellite images, "per-pixel" statistical classifiers (with and without layers of image texture), the geometric-optical canopy reflectance model of Li and Strahler (1985), and the texture classifier of Wang and He (1990). Likewise a number of types of imagery are being used, including LANDSAT Multispectral Scanner (MSS) and Thematic Mapper (TM) data, and SPOT High Resolution Visible (HRV) panchromatic data.

That such a variety of analysis techniques and image types are being used raises some important issues. Foremost among these is what impact image spatial resolution and image spectral properties have on the effectiveness of the methodologies. We initiated a study to evaluate several of the techniques being used and to determine the spectral and spatial properties of different types of imagery that best distinguish among conditions in late successional Douglas-fir / western hemlock (*Pseudotsuga menziesii / Tsuga heterophylla*) forest stands (Cohen and Spies, 1990). As stand structure is the most distinctive feature of different developmental stages and age classes of the region (Spies and Franklin, 1991), our efforts are concentrated on characterizing many stand structure attributes with the image data; for example, tree size, density, and basal area.

Initially, we used semivariograms to determine the spatial information content of aerial videography having resolutions, of 1 m, 10 m, and 30 m (Cohen et al., 1990). Results indicated that spatial measures of 10 m SPOT HRV panchromatic data should be useful for evaluation of stand attributes, whereas similar measures of TM 30 m multispectral data should not. In the research reported here, we examined both the spatial and spectral information contents of actual TM and HRV imagery. There were four main objectives.

1. To compare the utility of HRV and TM data for analysis of forest stand structural attributes. These are two of the principal forms of satellite data currently used, and likely to be used for similar analyses in the near future.
2. To evaluate image texture as a tool for analysis of forest stand attributes. Texture was chosen as the measure with which to capture image spatial information because it can be readily incorporated in a variety of image processing schemes.
3. To evaluate the effect of topography on satellite imagery. Topographic effects have been identified in the literature for a number of years as a major problem in image processing. Because an adequate solution to this problem has not been found, we thought it prudent to examine topographic effects on the utility of spectral and texture images to reliably quantify stand attributes.
4. To identify forest stand structural attributes that can be most reliably quantified using satellite imagery. Although this focus in remote sensing research in not new, there are certainly no definitive answers, as results among studies are highly variable. For this objective we wanted to construct models that could be used to estimate values of several stand attributes from image variables.

METHODS

Study Site and Ground Data Used

The geographic area of this research is the central Willamette National Forest located in the Oregon Cascade Mountains (approximately 122° west longitude and 44° north latitude). As a result of past fires, steeply dissected terrain, and intensive forest management practices, this landscape has a complex pattern of stand structural conditions. We focus on essentially closed canopy stands—those in which at least 80% of horizontal space is occupied by trees. This is because closed canopy conditions are of most current interest from ecological, wildlife, and management perspectives (see Spies and Franklin, 1991).

In closed canopy conifer forests of the region, structural conditions can be characterized on a continuum from simple in young, even-aged stands to complex in old-growth stands. Simply structured stands generally have a single canopy layer of similarly sized small trees with few canopy gaps, high tree density, and low basal area. Complex structured stands commonly have multiple canopy layers with numerous gaps and a variety of tree sizes, and relatively low tree density and high basal area in the upper canopy layers.

Stand-level ground data collected by Spies

and Franklin (1991), for all trees having a diameter at breast height (DBH) greater than 5 cm, were used in this study. From these data of over 200 stands, 41 closed canopy stands ranging in size from about 5 ha to 25 ha could be located in the satellite imagery used. For each stand, we calculated the attributes listed and described in Table 1. The two indices, SCI and CHD, were designed to capture diversity in the structure of a forest stand canopy. The CHD is based on theoretical concepts that describe the relative volume of "ecological space" occupied by trees in a stand (Spies and Cohen, 1991). Development of the SCI was inspired by the fact that most of the stand attributes evaluated are highly correlated in a given forest stand. Thus, the SCI is a means with which to capture in a single stand attribute the variability found in several stand attributes.

Canopy attributes related to stand structural complexity and to conditions in the upper canopy layers are most important in defining old-growth conditions (Franklin and Spies, 1991; Spies and Franklin, 1991). As such, in this study it is most important to accurately estimate the SCI and CHD, variability in tree sizes (DBH_{sd}, CD_{sd}, and HGT_{sd}), the mean size of trees in the upper canopy layers (DBH_u, CD_u, and HGT_u), and basal area and density of the upper canopy layers (DNY_u and BA_u). Less important are the attributes defining average structural conditions in the stands (DBH_{mn}, CD_{mn}, HGT_{mn}, DNY, and BA), as these are less indicative of stand age class and structural condition. One might consider stand age to be the most important stand attribute for this study. However, given variability in rates of stand development, age alone may not be very indicative of successional conditions and structural diversity, which are considered more important from an ecological perspective.

Image Data

An HRV 10 m panchromatic image (24 June 1989) and a TM 30 m multispectral image (30 July 1988) of the study area were acquired. To avoid problems associated with misregistration and resampling, the two scenes were not coregistered, but were processed separately. To achieve compression of the TM data volume, the six reflectance bands were transformed into the *bright-*

Table 1. Stand and Image Variables Used in Analyses

	Stand Variables[a]
DBH_{mn} DBH_{sd} DBH_u	Tree bole diameter (cm) measured at breast height
CD_{mn} CD_{sd} CD_u	Tree crown diameter (m) measured at maximum crown width
HGT_{mn} HGT_{sd} HGT_u	Tree height (m)
DNY DNY_u	Tree density (ha^{-1})
BA BA_u	Basal area ($m^2\ ha^{-1}$) of tree boles
AGE	Time since major disturbance (yr), such as clearcut or fire, and refers to the dominant Douglas-fir trees—age of stands 200 yr or older was estimated to the nearest 50 yr
SCI[b]	Structural Complexity Index
CHD[c]	Canopy Height Diversity Index
	Image Variables[d]
HRV_O HRV_T	Derived from SPOT High Resolution Visible panchromatic data
BRT_O BRT_T	Tassled Cap brightness derived from LANDSAT Thematic Mapper data
GRN_O GRN_T	Tassled Cap greenness derived from LANDSAT Thematic Mapper data
WET_O WET_T	Tassled Cap wetness derived from LANDSAT Thematic Mapper data

[a] Subscripts mn, sd, and u are, respectively, mean value for all trees, standard deviation of values for all trees, and mean value for trees in the upper canopy only (dominant, codominant, and emergent positions). Crown diameters and heights were based on both published (Spies et al., 1990) and unpublished species-specific equations that relate these variables to tree bole diameters.

[b] A measure developed as a part of this study to capture the structural diversity in a forest stand. Using all of the more than 200 stands sampled by Spies and Franklin (1991), a principal component analysis (SAS, 1991) was done using the variables DBH_{sd}, DBH_u, CD_{sd}, CD_u, HGT_{sd}, HGT_u, DNY_u, and BA_u. The SCI score for a stand is its score along the first principal component axis. The index varies between positive and negative six, with young stands having negative, and old stands having positive, scores.

[c] A measure developed as a part of this study to capture the height diversity in a forest stand (Spies and Cohen, 1991), calculated as $CHD = \sum_{i=1}^{n} H_i * P_i$, where n is the number of height classes, H_i is the relative height of height class i, calculated by dividing the upper limit of a height class by the upper limit of the lowest height class, and P_i is the percent canopy cover in height class i divided by a threshold value of 0.3. If P_i is greater than 1.0, then it is set equal to 1.0. Five height classes were used: 0–16 m, >16–32 m, >32–48 m, >48–64 m, and >64 m. The threshold value was arbitrarily chosen as a percentage of canopy cover in a layer that could be considered as fully functional ecologically. A young, even-aged stand of regenerating trees commonly has a CHD value near 1, whereas a complex old-growth stand commonly has a value between 7 and 15.

[d] Subscripts O and T refer to measures derived from the original and the texture images, respectively.

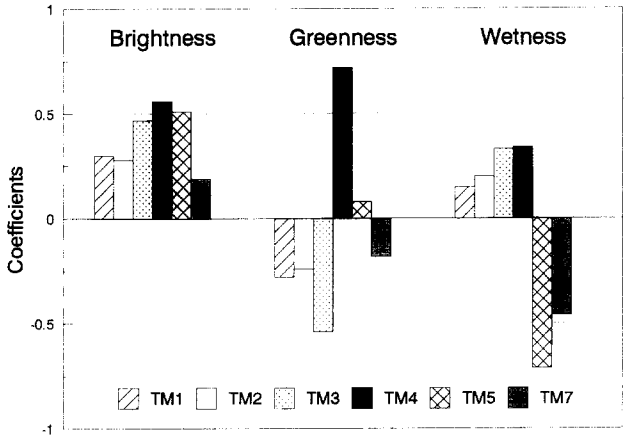

Figure 1. Coefficients for the first three features of the TM Tasseled Cap (adapted from Crist and Cicone, 1984).

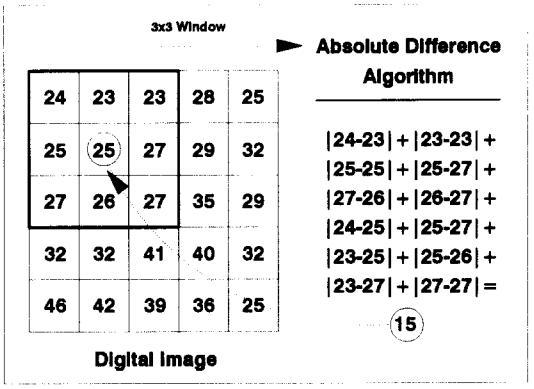

Figure 2. Example of how image texture was calculated using the absolute difference algorithm, given an image of digital numbers (DN) and a 3×3 pixel window as the basic spatial unit. The DN from each window are processed by the algorithm and the resulting texture number replaces the central pixel DN in the window.

ness, greenness, and *wetness* spectral indices of the TM Tasseled Cap (Crist et al., 1986). Brightness is a weighted sum of the six reflectance bands of the TM imagery, greenness is essentially a contrast between the near-infrared band (TM4) and the three visible bands (TM1, TM2, and TM3), and wetness is a contrast of midinfrared bands (TM5 and TM7) with the other four bands (Fig. 1).

Use of the terms brightness and greenness is well accepted within the remote sensing community; that is, there is a substantial body of literature suggesting that the names of these spectral features of TM data are consistent with the information they represent. In contrast, wetness has received little attention. Consequently, knowledge of whether this spectral feature actually responds to amounts of water in the ground scene is limited. This study provides an opportunity to determine the relationship of wetness with components of a conifer forest scene. A variety of other TM spectral indices are possible, such as the NDVI and the near-IR to red ratio (Cohen, 1991a). Likewise, we could evaluate the individual TM bands for their relationships with stand attributes. However, it was not our intent to test all possible spectral derivations in this study.

Texture images were created to capture the spatial information content of the satellite imagery. A wide variety of texture algorithms have been used to process digital imagery (Irons and Petersen, 1981; Gool et al., 1985; Mather, 1987). The *standard deviation* and *absolute difference* algorithms described by Rubin (1990) were considered for use here. They are computationally efficient, and we felt that they can be expected to capture the essence of the textural information contained in the imagery. Initial evaluation of these indicated that the absolute difference algorithm provided a greater dynamic range of texture information and therefore had potentially more discriminating power. Using this algorithm, and a moving 3×3 pixel window (Fig. 2), texture images were created from the brightness, greenness, and wetness images and from the HRV image.

The boundaries of each of the 41 stands in the HRV and Tasseled Cap imagery were digitized. Subsequently, the pixels corresponding to each stand were extracted from every image (the original HRV image, the brightness, greenness, and wetness images, and the four texture images). Plots of the pixels of the various stands from each image indicated that the texture and spectral values were normally distributed. This helped justify use of the mean values for the stands from each image in subsequent analyses.

Evaluation of Relationships and Model Construction

To determine the basic relationships among stand attributes and between stand attributes and the image variables, correlation coefficients were calculated. To determine the relative influence of topography on each spectral and texture variable, we calculated the coefficient of correlation for the relationship between the mean image value for a

stand and the cosine of the mean solar incidence angle (cos *i*, Smith et al., 1980) for the stand (from slope and aspect information collected on the ground). For all correlation analyses transformed variables were used where appropriate. Whether the stand variable, the image variable, neither variable, or both variables was / were transformed was dependent on the linearizing model which was appropriate and / or best fit the data (e.g., logarithmic, exponential, etc., Sabin and Stafford, 1990).

Linear regression models (SAS, 1991) were developed to estimate stand attributes from the mean values derived from the images. This is the most common use of regression analysis in remote sensing (Curran and Hay, 1986) and in the statistical literature this has been called inverse regression (as referenced in Cohen, 1991a). One should be advised, however, that estimation equations developed using inverse regression may be influenced by errors in measurement of both the dependent and independent variables (Curran and Hay, 1986). This problem is most important when models are developed using independent and dependent variables that are not well correlated with stand variables in model construction. As some stand attributes were not well correlated with any of the image variables, no models were constructed for those attributes. Attributes for which models were constructed include DBH_{sd}, DBH_u, HGT_{sd}, HGT_u, DNY_u, AGE, and SCI. Three types of models were built to estimate these stand attributes: 1) those using variables derived from the HRV data only (*HRV models*); 2) those using variables derived from the TM data only (*TM models*); and 3) those using variables derived from both image data sets (*combined models*).

Collection of Ground Radiometer Data

To assist in our interpretations of the results of this study, we collected bidirectional reflectance data of several scene components from a variety of forest stands in conditions similar to those of the study site. We used a Barnes Modular Multispectral Radiometer (MMR) equipped with filters that replicate the six TM reflectance bands. Our technique for collecting the data follows that described by Goward (1990) and is depicted in Figure 3. We obtained *in situ* reflectance measurements for Douglas-fir, western hemlock, and western redcedar (*Thuja plicata*) foliage, for foliage of herbaceous and hardwood plant species commonly found in the Douglas-fir / western hemlock zone, including vine maple (*Acer circinatum*), bigleaf maple (*Acer macrophyllum*), red alder (*Alnus rubra*), and bracken fern (*Pteridium aquilinum*), and for dead wood, tree bark, and epiphytic canopy lichens (several common species). We also collected spectra of the same components in complete shadows. Each measurement was refer-

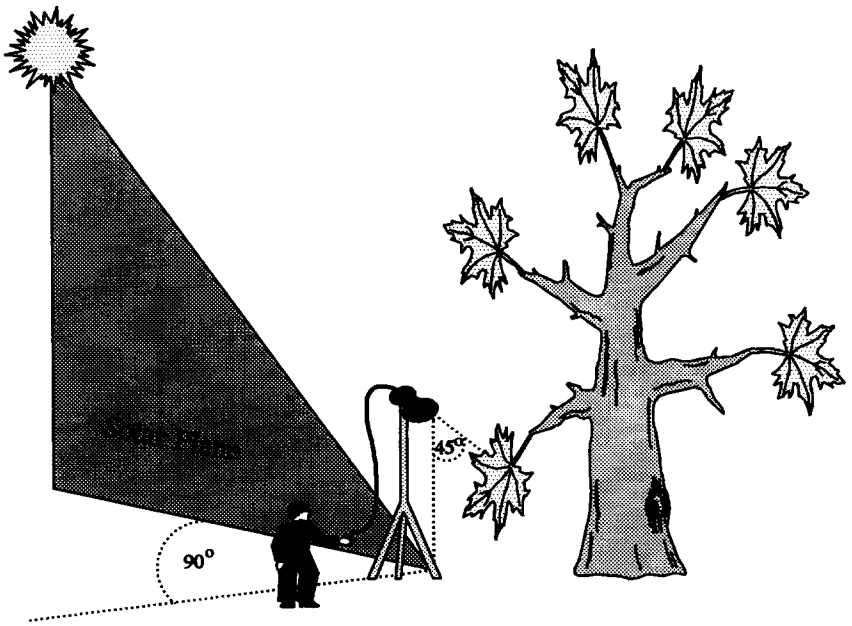

Figure 3. Physical setup for collection of the radiometer data (after Goward, 1990). The data were collected *in situ*, with the optical axis of the radiometer positioned perpendicular to the solar plane, 45° off-nadir, 3–4 m above ground, and 1 m from the target. The radiometer lens had a 15° field of view lens. All data were collected between 0900 and 1500 h local sun time on several different days in August 1990.

enced to a barium sulfate panel and was transformed into TM Tasseled Cap features using the coefficients for reflectance factor data (Crist, 1985).

RESULTS

Relationships among Stand Attributes

All stand attributes are positively related with each other except for density, which is negatively related to all other attributes (Table 2). Most of these relationships are strong (e.g., DBH_{sd} and DBH_u with other attributes), suggesting that they change in similar ways during forest succession. Obvious exceptions are the mean tree size attributes (DBH_{mn}, CD_{mn}, and HGT_{mn}), which are highly correlated with each other, but are generally not well correlated with most other attributes, except density (DNY). The latter is largely because the mean attribute values are highly dependent on the relative densities of trees in the understory (smaller trees) and overstory (larger trees). Density of understory trees is a highly variable parameter in more complex stands, and is dependent on stand history and cover in the upper canopy layers. That the mean attributes are highly correlated with each other is undoubtedly in part a function of the fact that height and crown diameter are predicted from DBH. Basal area (BA) of a stand is only moderately correlated with the other attributes. This is likewise a function of the relationship between density and mean tree size, in that basal area is essentially the product of these attributes. It is important to point out that when only the trees of the upper canopy layers are considered, tree sizes (DBH_u, CD_u, and HGT_u) are highly correlated with most of the other attributes, as is density (DNY_u). There is little difference between basal area of the entire stand and basal area of the upper canopy layers (BA_u).

Stand Attributes in Relation to Image Variables

Mean stand texture number of the HRV data (HRV_T) exhibited strong relationships with the stand attributes (Table 3). For all but the mean tree size attributes (DBH_{mn}, CD_{mn}, HGT_{mn}) and DNY the absolute value of the coefficient of correlation ($|r|$) was between 0.72 and 0.88. This indicates that texture images of 10 m resolution satellite data capture the relative degrees of spatial variability of sunlight and shadow patterns associated with stand complexity, as indicated in our semivariogram study (Cohen et al., 1990). There was essentially no relationship between the stand attributes and the mean digital number from the original HRV data (HRV_o).

Mean stand wetness (WET_o) was the TM variable most strongly correlated with all stand attributes ($0.51 < |r| < 0.90$). Mean stand brightness (BRT_o) and mean stand greenness (GRN_o) were poorly correlated with all attributes. As with HRV_T, the attributes having the strongest relationships ($0.81 < |r| < 0.90$) with WET_o were those describing tree size variability (DBH_{sd} and HGT_{sd}), tree sizes of the upper canopy layers

Table 2. A Correlation Matrix for the Stand Attributes[a]

DBH_{mn}	DBH_{sd}	DBH_u	CD_{mn}	CD_{sd}	CD_u	HGT_{mn}	HGT_{sd}	HGT_u	DNY	DNY_u	BA	BA_u	AGE	SCI	CHD	
1.00	0.61	0.65	0.87	0.20	0.52	0.95	0.53	0.74	−0.80	−0.56	0.69	0.71	0.28	0.62	0.54	DBH_{mn}
	1.00	0.98	0.76	0.80	0.93	0.45	0.96	0.94	−0.70	−0.81	0.78	0.79	0.79	0.99	0.83	DBH_{sd}
		1.00	0.77	0.75	0.91	0.49	0.92	0.96	−0.70	−0.80	0.77	0.76	0.72	0.97	0.84	DBH_u
			1.00	0.53	0.76	0.76	0.65	0.80	−0.77	−0.66	0.66	0.67	0.57	0.77	0.56	CD_{mn}
				1.00	0.89	0.02	0.77	0.65	−0.39	−0.64	0.41	0.42	0.79	0.81	0.57	CD_{sd}
					1.00	0.37	0.88	0.88	−0.66	−0.81	0.64	0.65	0.87	0.95	0.76	CD_u
						1.00	0.40	0.64	−0.79	−0.51	0.56	0.59	0.15	0.48	0.45	HGT_{mn}
							1.00	0.92	−0.71	−0.82	0.74	0.76	0.74	0.96	0.81	HGT_{sd}
								1.00	−0.82	−0.87	0.79	0.79	0.68	0.97	0.85	HGT_u
									1.00	0.82	−0.54	−0.61	−0.49	−0.75	−0.68	DNY
										1.00	−0.52	−0.55	−0.67	−0.87	−0.71	DNY_u
											1.00	0.98	0.55	0.77	0.64	BA
												1.00	0.56	0.78	0.65	BA_u
													1.00	0.80	0.57	AGE
														1.00	0.83	SCI
															1.00	CHD

[a] See Table 1 for description of variables.

(DBH_u, CD_u, HGT_u), DNY_u, AGE, and the SCI. As wetness is a spectral rather than a spatial measure, it should not be expected to respond to patterns of sunlight and shadow in a forest stand. Furthermore, 30 m spatial resolution imagery is too coarse for within stand pattern analysis under the conditions of this study (Cohen et al., 1990). This is most likely why the mean stand texture numbers from the brightness (BRT_T), greenness (GRN_T), and wetness (WET_T) texture images exhibited poor relationships with the stand attributes. Apparently, wetness responds to some other factor in the forest canopy.

For nine of the 16 stand attributes examined HRV_T was more strongly correlated than WET_O; the exceptions were the mean tree size variables (DBH_{mn}, CD_{mn}, and HGT_{mn}), the density variables (DNY and DNY_u), and stand age. The correlations of HRV_T and WET_O with CD_u were the same. For a given stand attribute the difference between the correlation coefficients for HRV_T and WET_O was less than 0.08. In general, the difference was less, indicating that there should not be much difference in accuracy of estimating stand attributes whether TM wetness or HRV texture is used. The CHD was not strongly related to either HRV_T or WET_O. The SCI exhibited considerably stronger relationships than the CHD with both HRV_T and WET_O.

Topographic Influences on the Image Data

The image variables HRV_O and mean stand brightness (BRT_O) and greenness (GRN_O) were more strongly related to topography (the cosine of the solar incidence angle—cos *i*) than to any of the stand attributes (Table 3). This is the most probable reason why these variables were not well correlated with any of the stand attributes. The variables HRV_T and WET_O were not well correlated with cos *i*. This permitted the stand structural mechanisms driving these image variables to dominate their response. The variables BRT_T, GRN_T, and WET_T were not dominated by topography, but as previously stated they were not dominated by stand structural conditions either.

Figure 4 illustrates the influence of topography on image data. On sunlit slopes brightness and greenness, and to a lesser extent the HRV data, captured the spectral variability associated with different degrees of canopy structural complexity. However, on slopes facing away from the sun, stands with canopies with intermediate and complex structures are generally indistinguishable from each other. Also, stands with a simple canopy structure facing away from the sun have ranges of brightness, greenness, and HRV values that are similar to those of stands with an intermediate canopy complexity facing toward the sun.

Table 3. Absolute Value of Correlation Coefficients for the Relationships of Stand Structural Attributes and a Topographic Variable (cos *i*) with Variables Derived from the Satellite Data[a]

Stand Variable	HRV_O	HRV_T	BRT_O	GRN_O	WET_O	BRT_T	GRN_T	WET_T
DBH_{mn}	*	0.55	0.44	0.44	−0.60	*	*	*
DBH_{sd}	*	0.88	0.53	0.55	−0.87	*	*	*
DBH_u	*	0.88	0.43	0.47	−0.87	*	*	*
CD_{mn}	*	0.67	0.33	0.35	−0.69	*	*	*
CD_{sd}	*	0.72	0.27	0.25	−0.67	*	*	*
CD_u	*	0.88	0.42	0.27	−0.88	*	*	*
HGT_{mn}	*	0.45	0.37	0.37	−0.51	*	*	*
HGT_{sd}	*	0.88	0.30	0.42	−0.81	*	*	*
HGT_u	*	0.86	0.35	0.43	−0.85	*	*	*
DNY	*	−0.62	0.49	0.51	0.69	*	*	*
DNY_u	*	−0.84	0.39	0.51	0.87	*	*	*
BA	*	0.73	0.53	0.52	−0.69	*	*	*
BA_u	*	0.73	0.47	0.53	−0.71	*	*	*
AGE	*	0.87	0.55	0.63	−0.90	*	*	*
SCI	*	0.88	0.55	0.65	−0.86	*	*	*
CHD	*	0.75	0.53	0.54	−0.69	*	*	*
cos *i*[b]	0.51	*	0.63	0.68	*	*	*	*

[a] See Table 1 for descriptions of stand attributes. * indicates <0.25.
[b] Cosine of the solar incidence angle, based on slope and aspect of the location of a forest stand (Smith et al., 1980).

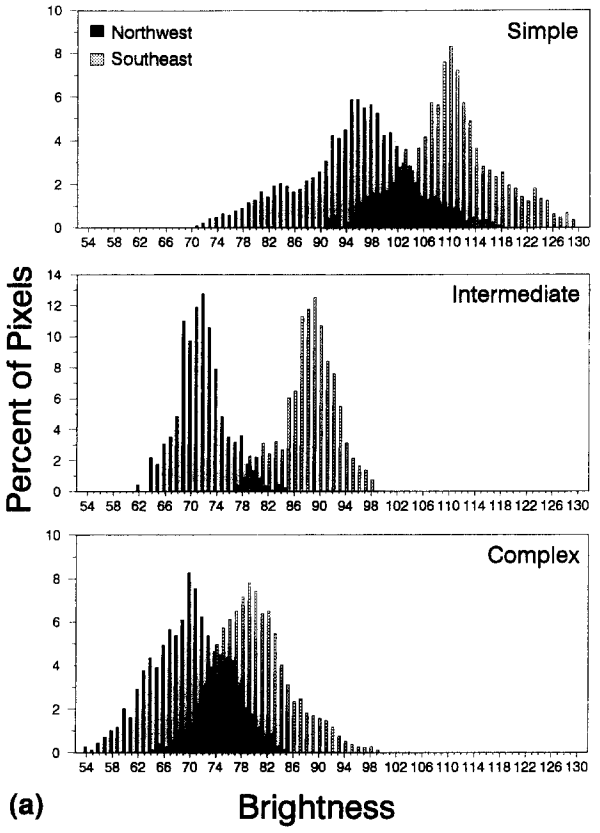
Northwest
Southeast
Simple
Intermediate
Complex
Percent of Pixels
(a)
Brightness

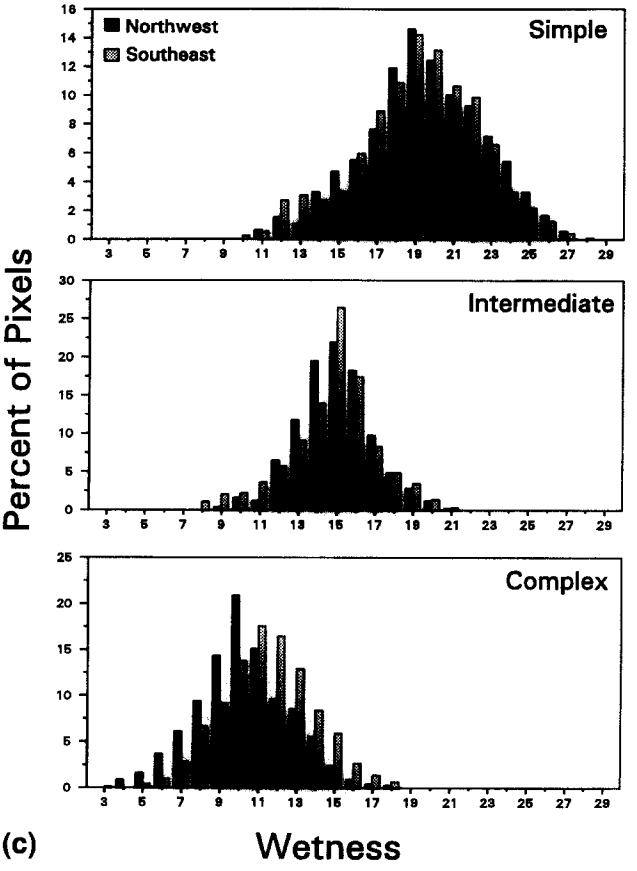
Northwest
Southeast
Simple
Intermediate
Complex
Percent of Pixels
(c)
Wetness

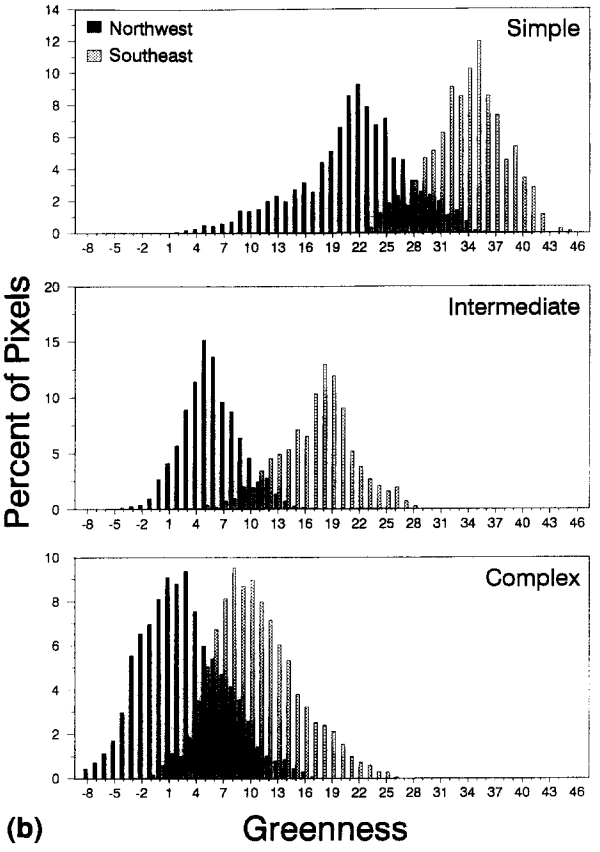
Northwest
Southeast
Simple
Intermediate
Complex
Percent of Pixels
(b)
Greenness

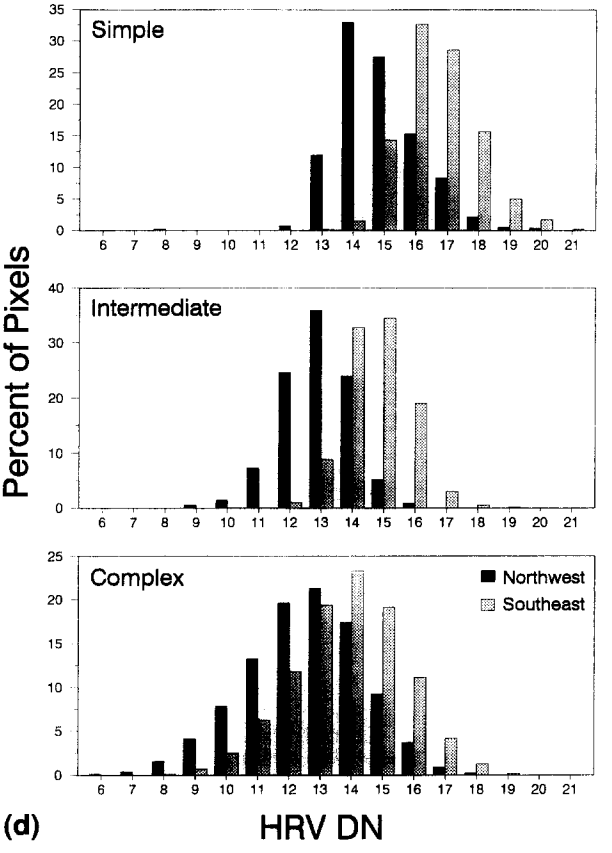
Simple
Intermediate
Complex
Northwest
Southeast
Percent of Pixels
(d)
HRV DN

Figure 4.

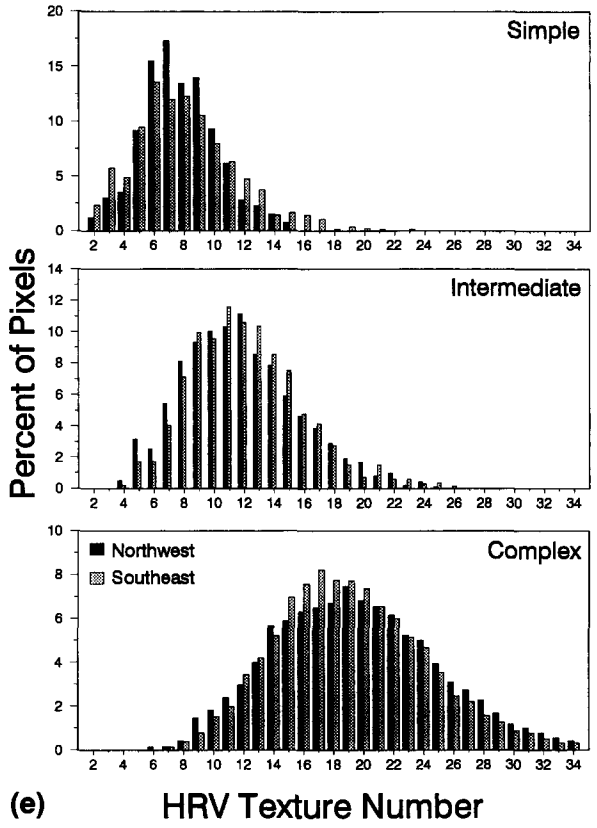

Figure 4. Histograms of pixels values from a) brightness and b) greenness, c) wetness, d) original HRV, and e) HRV texture images for three coarse levels of canopy structural complexity on slopes facing away from the sun (Northwest) and slopes facing toward the sun (Southeast). Three separate stands were included in each histogram.

Furthermore, the ranges of brightness, greenness, and HRV values associated with the complex canopy class on a sunlit slope falls within the full range of values associated with stands having intermediate canopy complexities regardless of slope. These topographic effects are not apparent in HRV texture and TM wetness.

The probable reasons why HRV_T and WET_O are not very sensitive to topography may not be readily apparent. For HRV_T, a logical explanation is that local variability is evaluated rather than local means. For WET_O, the apparent reason is that wetness is similar to the third principal component of TM imagery (Horler and Ahern, 1986). The first two components, brightness and greenness, capture most of the variability in the spectral values. This includes topographic effects which tend to dominate the spectral signal of individual bands of satellite data in mountainous terrain (Walsh, 1980; 1987; Justice et al., 1981). Wetness captures the next degree of spectral variability, which apparently is largely a function of stand structure.

Regression Models

The regression models (Table 4) reveal that by careful selection of appropriate image variables, reliable estimates of a variety of stand attributes can be obtained. The variable HRV_T in each of the HRV models accounts for at least 70% of the variation in the stand attribute values. The same is true for WET_O in the TM models, with the exception of the model for HGT_{sd}. In general, it appears that using either TM wetness or HRV texture will yield results that are equally reliable when estimating stand attributes. It is important to note that both the HRV and TM models for SCI appear to be as reliable as those for estimating the other attributes. This means a single variable representing structural complexity in closed canopy forest stands can be remotely sensed, which has significant implications for landscape or regional analyses of biodiversity, wildlife habitat, and the like.

All combined models explain more of the variation in stand attribute values than either the

Table 4. Regression Models Constructed to Estimate Selected Stand Attributes from Image Variables[a]

Dependent Variable	*Independent Variables and Coefficients*	*Model r^2*	*RMSE*
	HRV Models		
$Ln(DBH_{sd})$	$-0.394 + 1.493*Ln(HRV_T)$	0.77	0.25
$Ln(DBH_u)$	$0.340 + 1.496*Ln(HRV_T)$	0.77	0.25
HGT_{sd}	$-18.42 + 13.85*Ln(HRV_T)$	0.77	2.31
HGT_u	$-41.92 + 41.91*Ln(HRV_T)$	0.74	0.19
$Ln(DNY_u)$	$9.985 - 1.970*Ln(HRV_T)$	0.70	0.39
Ln(AGE)	$-1.738 + 2.726*Ln(HRV_T)$	0.76	0.46
SCI	$-8.232 + 0.605*HRV_T$	0.78	1.23
	TM Models		
$Ln(DBH_{sd})$	$6.450 - 0.216*WET_O$	0.76	0.25
$Ln(DBH_u)$	$7.177 - 0.216*WET_O$	0.76	0.24
HGT_{sd}	$43.13 - 1.873*WET_O$	0.66	2.71
$Ln(HGT_u)$	$5.542 - 0.135*WET_O$	0.72	0.17
$Ln(DNY_u)$	$0.927 + 0.288*WET_O$	0.74	0.34
Ln(AGE)	$11.16 - 0.422*WET_O$	0.81	0.41
SCI	$14.84 - 1.071*WET_O$	0.74	1.29
	Combined Models		
$Ln(DBH_{sd})$	$2.898 + 0.829*Ln(HRV_T) - 0.114*WET_O$	0.83	0.21
$Ln(DBH_u)$	$3.760 + 0.797*Ln(HRV_T) - 0.117*WET_O$	0.83	0.21
HGT_{sd}	$0.956 + 9.840*Ln(HRV_T) - 0.655*WET_O$	0.79	2.19
$Ln(HGT_u)$	$3.655 + 0.440*Ln(HRV_T) - 0.080*WET_O$	0.78	0.15
$Ln(DNY_u)$	$4.598 - 0.857*Ln(HRV_T) + 0.182*WET_O$	0.79	0.32
Ln(AGE)	$5.886 + 1.230*Ln(HRV_T) - 0.270*WET_O$	0.86	0.36
SCI	$2.554 + 0.353*Ln(HRV_T) - 0.531*WET_O$	0.83	1.04

[a] Descriptions and units of dependent variables are shown in Table 1.

HRV or TM models. This is largely because two important predictor variables were used in the combined models and only one was used in the other types of models. Also, these models contain predictor variables that appear to respond to different mechanisms in the forest canopy. That is, HRV_T contains spatial information at a scale of resolution appropriate to certain canopy processes, and WET_O contains spectral information appropriate for detecting different canopy processes.

Radiometer Reflectance Measurements

For this study we focus only on the calculated wetness values from the radiometer data. Additionally, for practical purposes, the spectra for some components that are commonly found in close association have been grouped together (e.g., herbaceous and hardwood foliage components).

The locations of these groups of scene component reflectance spectra along the wetness axis are shown in Figure 5. All shades components have very similar wetness values, as indicated by the lack of significant variation. Also, shaded data have the highest wetness values. Sunlit western hemlock and Douglas-fir foliage are virtually indistinguishable, and the wetness values of these two components are not much different qualitatively from those of shaded components. As might be expected, background vegetation is highly variable, but, on average, it has the lowest values. The combined signal for canopy lichen, bark, and dead wood is less variable than background vegetation, but has a similar mean value. Western redcedar spectra have intermediate wetness values, relative to the other components.

DISCUSSION

Utility of Texture in Relation to Image Spatial Resolution

If only texture information is considered, then HRV 10 m imagery is clearly more useful for evaluation of stand structural attributes than is TM 30 m imagery. To better understand why, we

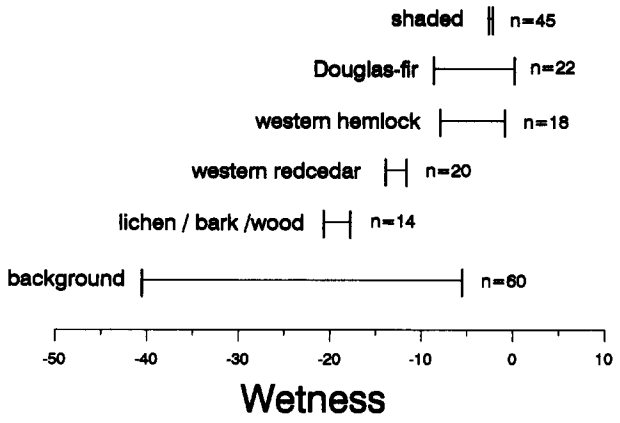

Figure 5. Plots of means and standard errors of scene components spectra collected with the ground radiometer: sunlit components (Douglas-fir, western hemlock, and western redcedar foliage, canopy lichen / bark / dead wood, and background herbaceous and hardwood foliage) and all shaded components.

refer to the work of Woodcock and Strahler (1987), who state that the value of texture measures in image processing depends on whether image resolution cells are smaller than the elements of interest in the scene. The basic element of interest in our study is the individual tree, or as viewed from above, the tree crown. In the young, simply structured Douglas-fir / western hemlock stands evaluated here the dominant tree crown is approximately 5 m in width, whereas in mature (moderately complex) and old-growth (complex) stands it is rougly 10 m and 15–20 m, respectively (Cohen et al., 1990; Spies et al., 1990). Even though young closed canopy stands have tree crowns that are subpixel size, the fact that more complex stands have numerous tree crowns that are at least as large as the pixels helps to discriminate simply structured stands from more complex stands. Likewise, because stands with moderately complex structures have tree crowns roughly equivalent in size to the image pixels and complex structured stands have crowns larger than one pixel, these two conditions also are distinguishable using textural measures of 10 m data. With the 30 m data at least two or three large trees generally appear in many pixels, severely diminishing the ability of TM texture to discriminate. Note, however, that in stands not having closed canopies—that is, where trees are found in clumps and the background has drastically different spectral properties—this logic may not hold.

Relative Value of TM and HRV Spectral Information

If only spectral information is considered, TM data are more useful than panchromatic HRV data, regardless of whether the brightness, greenness, or wetness spectral features of the TM data are used. As HRV imagery contains information from the visible portion of the electromagnetic spectrum only, where vegetation absorbs almost all energy and atmospheric scattering is greatest, this is no surprise. In contrast, TM data is multispectral and contains information from the infrared portion of the spectrum where most of the spectral differences in vegetation occur and atmospheric effects are less evident. An apparent reason for the value of wetness over brightness and greenness is the relative lack of sensitivity to topography that wetness exhibits. As each of the individual bands of TM data also are strongly influenced by topography, the importance of using appropriate image spectral transformations is readily apparent.

Mechanisms Driving the Response of TM Tasseled Cap Wetness

There is both theoretical and empirical evidence indicating that water volume and degree of shadowing are the primary driving forces in the response of wetness to variations in scene components. Thus, it is with these two phenomena that we begin this part of our investigation.

Wetness is a contrast of TM Bands 5 and 7 with the other four TM bands (Fig. 1). Bands 5 and 7 are in the portion of the electromagnetic reflectance spectrum where water is most absorptive of incident energy (Curcio and Petty, 1951). Using a stochastic model, Tucker (1980) developed the theoretical basis for plant leaf water absorption in these two TM bands. The studies just cited, as well as those by Crist et al. (1986), led to the naming of this spectral feature. Crist et al. (1986) and Musick and Pelletier (1988) demonstrated that wetness responds to changes in soil moisture and Cohen (1991a) demonstrated that wetness is responsive to changes in water content of leaf samples. The relationship between wetness and amount of water is positive, since with an increase in amount of water more energy is absorbed in TM5 and TM7 relative to TM Bands 1–4 (Fig. 1).

Horler and Ahern (1986) were the first to report that a "wetnesslike" feature of TM data—they used the term "SWIRness"—is responsive to variations in conifer canopy structure. Their results indicate that tree density and related amounts of shadow in TM-sized resolution elements control the wetness response. Crist et al. (1986) and Kimes et al. (1986) explain the theoretical basis for the response of wetness to shadow. Because of the inverse relationship between wavelength and atmospheric scattering, shadowed areas of a scene should receive more energy in TM Bands 1–4 and less in Bands 5 and 7. Thus, since wetness is a contrast of Bands 5 and 7 (negative coefficients) with Bands 1–4 (positive coefficients), greater proportions of shadow should result in greater values of wetness. Further evidence is provided by the fact that low energy reflecting panels have higher values of wetness than high energy reflecting panels under uniform experimental conditions (Crist et al., 1986). We demonstrated in this study with our ground radiometer data that shaded components have greater wetness values than sunlit components.

Given the positive relationship that wetness exhibits in response to amount of water and degree of shadowing, we now turn our attention to the structure of forest canopies. In forest canopies the amount of "water-filled" foliage viewed by the sensor is inextricably linked to the degree of canopy shadowing. Cohen et al. (1990) discuss in detail the shadow patterns found in the conifer forest stands of the Pacific Northwest, indicating that, in general, the older and more complex the stand, the greater the proportion of shadow present. Because the amount of shadow is greater in more complex stands, we can safely assume that the amount of foliage per unit area visible to the TM sensor is less in these stands than in closed canopy stands with more simple structures. Thus, there are contradictory trends here: With increased stand structural complexity, wetness should increase due to greater proportions of canopy shading; however, wetness should decrease due to less foliage being viewed by the sensor. In reality, however, wetness values for sunlit Douglas-fir and western hemlock foliage and for shaded components are very similar (Fig. 5), depriving this whole argument of practical significance. As a result, we must look elsewhere for the mechanism driving the wetness response in closed canopy forests.

The controlling factor may be in part the amount of age-related canopy die-back, tree death, and increase in epiphytic lichen. With increasing age, individual tree crowns in the upper layers begin to die, thereby losing foliage and exposing bark and dead wood. At the same time, canopy lichens begin to grow in increasingly greater amounts. The tops of many of the trees break, as others become snags. Cohen (1991b) demonstrated that woody and other nongreen plant materials have wetness values considerably lower than does green foliage. The same result can be inferred from the spectra of Guyot et al. (1989) and Elvidge (1990) indicating that dry components and nongreen and light-green nonfoliage materials have higher reflectance in the TM5 and TM7 region of the electromagnetic spectrum relative to reflectance in the region of TM1–TM4 than does green foliage. Our radiometer data from this study incidate that canopy lichen, bark, and dead wood have lower wetness values than sunlit Douglas-fir and western hemlock foliage and all shaded components (Fig. 5). Additionally, older stands typically contain western redcedar in the upper canopy layers, and sunlit foliage of this species also generally has lower wetness values than the sunlit Douglas-fir and western hemlock foliage and all shaded components. Because wetness has an inverse relationship with structural complexity (Tables 3 and 4), we hypothesize that the amount of canopy lichen, bark, and dead wood, and to a smaller degree the amount of western redcedar present in the upper canopy layers, is largely responsible for controlling the wetness response in the closed canopy stands evaluated here. This hypothesis is supported by evidence that the inner half-radius of an old Douglas-fir tree crown can be covered by as much as 75% canopy lichen, as viewed from above (Bruce McCune, personal communication). Younger, more vigorous trees typically have little or no lichen in their crowns. An unknown in this discussion pertains to the background vegetation. It is highly variable in both the wetness values it exhibits and the degree to which it is illuminated in simply and more complex structured stands. Given these large degrees of variability, we consider the presence of background materials "noise" in the wetness signal.

If our hypothesis for the response of wetness to stand senescence holds, the question must be asked if use of the term wetness is appropriate?

Viewing a wetness image of a landscape containing distinct water bodies readily reveals that water has only a medium value. This alone is cause for dropping use of the term wetness and searching for an alternative, more appropriate name for this important spectral feature of TM data; one that is robust enough to describe a general vegetation condition, or process, across numerous ecosystem types.

In conifer forest scenes, clearcuts have the lowest wetness values, whereas young, closed canopy stands have the highest values. After this peak in wetness, as the forest stands begin to mature their wetness values become lower due to increasing amounts of scene components other than green foliage. In agricultural scenes, similar canopy maturity patterns occur, and the response of wetness is the same. Bare ground can be expected to have the lowest wetness values (Crist et al., 1986), wetness increases until a crop reaches maximum green foliage cover and uniformity, and then begins to decrease as the crop matures. The same should hold true for rangelands and other vegetation types. Thus, we propose use of the term "maturity" to describe the response of the third feature of the TM Tasseled Cap.

Topographic Effects on the Estimation of Stand Attributes

Evaluation of forested landscapes with remote sensing imagery goes back to the early days of the LANDSAT program. Iverson et al. (1989) review many of these studies in detail. Additional research not reviewed by Iverson et al. include studies of site productivity (Tom and Miller, 1979), leaf biomass (Franklin and Hiernaux, 1991), land cover stratification (Strahler, 1981; Franklin, 1991), leaf area index (Spanner et al., 1990), timber volume (Franklin et al., 1986), tree species (Conese et al., 1988), canopy closure (Butera, 1986), canopy reflectance modeling (Li and Strahler, 1985; Franklin and Strahler, 1988; and Franklin et al., 1991), and stand age, basal area, and tree diameter, height, and density (Johnson et al., 1979; Horler and Ahern, 1986; Danson, 1989; and De Wulf et al., 1990).

Among studies, there have been differing degrees of success, depending on geographic location, technique employed, image data used, and forest variable evaluated. A variety of problems have been identified, including the effects of shadows and scene background variability (Colwell, 1974; De Wulf et al., 1990; Spanner et al., 1990), solar illumination angle and variable topography (Walsh 1980; 1987; Justice et al., 1981; Teillet et al., 1982), spatial heterogeneity of image digital numbers within a stand (Conese et al., 1988), and interactions between the forest attributes of interest and image spatial resolution (Woodcock and Strahler, 1987; Atkinson and Danson, 1988). Of all the problems identified, topographic variability often has the greatest impact in mountainous terrain on per-pixel classifiers of image data. Walsh (1980; 1987) and Conese et al. (1988) demonstrated that variables such as slope, aspect, or cosine of the solar incidence angle are often more strongly correlated with image data than are forest stand variables. We have confirmed this here. Furthermore, many of the other problems identified are actually caused by topographic variation. For example, variations in shadow patterns among forest stands and proportions of scene background visible to a sensor can be expected to vary greatly among nearly identical forest stands simply because they reside on different slopes or aspects.

Given that it is essential to minimize topographic effects in satellite imagery for analysis of forest conditions, what are the choices currently available? With the advent of digital elevation models (DEM) numerous investigators have attempted to solve problems associated with topography by applying corrections for cosine of the solar illumination angle (Smith et al., 1980; Holben and Justice, 1980; Colby, 1991), or one of numerous other techniques (Civco, 1989; Pouch and Campagna, 1990). Results from such corrections are highly variable however (Ahern et al., 1987; Proy et al., 1989), suggesting that they are inappropriate for general application and that the phenomenon is not well understood. We demonstrated here that perhaps a more valuable solution is to use image derivatives that are relatively insensitive to topography and that the appropriate image derivates will, of course, vary with image and scene spectral and spatial characteristics.

CONCLUSIONS

Both LANDSAT TM and SPOT HRV panchromatic images are valuable data sources for analysis of Douglas-fir / western hemlock forest stand

structural attributes in the Pacific Northwest region of the United States. Many attributes, such as tree size variability and mean size and density of trees in the upper canopy layers, are highly correlated and are thus good indicators of structural complexity. As a result, these attributes can be estimated by remote sensing data with roughly the same degree of reliability, as can a structural complexity index that capitalizes on this correlation.

Overall, there appears to be little difference between the two types of imagery used here, in terms of the reliability of attribute estimates derived from them. However, with TM data it is the spectral properties of the imagery (e.g., vegetation indices) that must be used, and with HRV data it is the spatial properties (e.g., image texture) that are more valuable. The HRV data lack desired spectral resolution, but have a spatial resolution fine enough to capitalize on sunlight and shadow patterns that are characteristic of different degrees of structural complexity. Spatial measures of TM data provide little or no stand structure information for the closed canopy conditions analyzed because the spatial resolution of the data is inappropriate. The Tasseled Cap wetness spectral feature of TM data is substantially more valuable than the brightness or greenness spectral features more commonly used. This is primarily because wetness is insensitive to topographically induced illumination angle—which dominates the brightness and greenness indices derived from TM imagery obtained over complex terrain—and is apparently quite sensitive to structural features associated with canopy maturity (e.g., amount of dead wood and epiphytic lichen in the upper canopy layers). Likewise, it is the insensitivity of HRV texture to topography that permits its usage for analysis of stand structure in the forests of the Pacific Northwest. We propose that the term "maturity" replace the term wetness, as we believe that the successional stage of development in a plant canopy is the primary mechanism driving this TM spectral feature in a variety of ecosystem types. Of course, this hypothesis needs to be substantiated.

Although the use of both spatial and spectral measures in unison can be expected to improve the accuracy of estimation, compared to use of spectral or spatial measures alone, the increase in accuracy is generally less than 5–10%. This has been demonstrated here, as well as by others (Teillet et al., 1981; Franklin et al., 1986; Franklin and Peddle, 1989; 1990; Peddle and Franklin, 1991). For the forest conditions evaluated here, both HRV and TM data would be required to achieve this improved accuracy, and the additional cost of two data sets, relative to the improved results expected, does not appear practical. Furthermore, the problem associated with misregistration would potentially offset any gains otherwise made. The use of multispectral HRV data is an alternative option; but its spatial resolution is 20 m, and it does not have the spectral bands needed to calculate a wetness features. Landsat 6 will have the Enhanced TM (ETM) sensor that will include a 15 m panchromatic channel. As a result, ETM will likely be the next most powerful source of satellite imagery for analysis of forest stand attributes in the Pacific Northwest.

The research reported here indicates that reliable stand-level information, as well as how stand conditions are distributed across a landscape, can be derived from satellite remote sensing data. We are currently in the process of applying regression models developed here across large portions of the Douglas-fir / western hemlock zone in Oregon. Our method involves use of a clustering algorithm to identify closed canopy stands in the imagery, and then applying the regression models to those stands. This gives us the opportunity to evaluate spatial patterns of stand structure across relatively large landscapes.

Whereas historically the dominant focus was on timber production, in recent years the focus was transformed into one in which whole ecosystems and their structure and function are equally important. As this "new" ecological focus crystallizes, there is an increasing need to view not just the individual forest stands, but to study how the stands form patterns across the landscape. Consequently, land managers are more in need of sources of extensive information then ever before, and are increasingly using remotely sensed data to fulfill that need.

This research was funded in part by the Pacific Northwest Region of the Forest Service, the H. J. Andrews LTER, and NASA Grant NAGW-1460. We gratefully acknowledge the valuable programming assistance of Barbara Marks and Gody Spycher and all individuals involved in collection and entry into a computer of the ground data used. We appreciate the

statistical advice of Tim Max and want to express our thanks to those who critically reviewed this manuscript, including Claire Hay, John Runyon, David Wallin, and Gay Bradshaw. Special thanks to the reviewers for their constructive criticism.

REFERENCES

Ahern, F. J., Brown, R. J., Cihlar, J., et al. (1987), Radiometric correction of visible and infrared remote sensing data at the Canada Centre for Remote Sensing, *Int. J. Remote Sens.* 8:1349–1376.

Atkinson, P. M., and Danson, F. M. (1988), Spatial resolution for remote sensing of forest plantations, in *Proceedings, IGARSS '88 Symposium*, Edinburgh, Scotland, 13–16 September 1988, ESA Publ. Division, pp. 221–223.

Butera, M. K. (1986), A correlation and regression analysis of percent canopy closure versus TMS spectral response for selected forest sites in the San Juan National Forest, Colorado, *IEEE Trans. Geosci. Remote Sens.* GE-24:122–129.

Civco, D. L. (1989), Topographic normalization of Landsat Thematic Mapper digital imagery, *Photogramm. Eng. Remote Sens.* 55:1303–1309.

Cohen, W. B. (1991a), Response of vegetation indices to changes in three measures of leaf water stress, *Photogramm. Eng. Remote Sens.* 57:195–202.

Cohen, W. B. (1991b), Chaparral vegetation reflectance and its potential utility for assessment of fire hazard, *Photogramm. Eng. Remote Sens.* 57:203–207.

Cohen, W. B., and Spies, T. A. (1990), Remote sensing of canopy structure in the Pacific Northwest, *Northwest Environ. J.* 6:415–418.

Cohen, W. B., Spies, T. A., and Bradshaw, G. A. (1990), Semivariograms of digital imagery for analysis of conifer canopy structure, *Remote Sens. Environ.* 34:167–178.

Colby, J. D. (1991), Topographic normalization in rugged terrain, *Photogramm. Eng. Remote Sens.* 57:531–537.

Colwell, J. E. (1974), Vegetation canopy reflectance, *Remote Sens. Environ.* 3:175–183.

Conese, C., Maracchi, G., Miglietta, F., Maselli, F., and Sacco, V. M. (1988), Forest classification by principal component analysis of TM data, *Int. J. Remote Sens.* 9: 1597–1612.

Crist, E. P. (1985), A TM Tasseled Cap equivalent transformation for reflectance factor data, *Remote Sens. Environ.* 17:301–306.

Crist, E. P., and Cicone, R. C. (1984), A physically-based transformation of Thematic Mapper data—the TM Tasseled Cap, *IEEE Trans. Geosci. Remote Sens.* GE-22:256–263.

Crist, E. P., Laurin, R., and Cicone, R. C. (1986), Vegetation and soils information contained in transformed Thematic Mapper data, in *Proceedings, IGARSS '86 Symposium*, Zürich, Switzerland, 8–11 September 1986, ESA Publ. Division, SP-254, pp. 1465–1470.

Curcio, J. A., and Petty, C. C. (1951), Extinction coefficients for pure liquid water, *J. Opt. Soc. Am.* 41:302–303.

Curran, P. J., and Hay, A. M. (1986), The importance of measurement error for certain procedures in the remote sensing at optical wavelengths, *Photogramm. Eng. Remote Sens.* 52:229–241.

Danson, F. M. (1989), Factors affecting the remotely-sensed response of coniferous forest canopies, Ph.D. dissertation, Department of Geography, University of Sheffield, England.

De Wulf, R. R., Goossens, R. E., DeRoover, B. P., and Borry, F. A. (1990), Extraction of forest stand parameters from panchromatic and multispectral SPOT-1 data, *Int. J. Remote Sens.* 11:1571–1588.

Elvidge, C. D. (1990), Visible and near infrared reflectance characteristics of dry plant materials, *Int. J. Remote Sens.* 11:1775–1796.

Franklin, J. (1991), Land cover stratification using Landsat Thematic Mapper data in Sahelian and Sudanian woodland and wooded grassland, *J. Arid Environ.* 20:141–163.

Franklin, J., and Hiernaux, P. H. Y. (1991), Estimating foliage and woody biomass in Sahelian and Sudanian woodlands using a remote sensing model, *Int. J. Remote Sens.* 12: 1387–1404.

Franklin, S. E., and Peddle, D. R. (1989), Spectral texture for improved class discrimination in complex terrain, *Int. J. Remote Sens.* 10:1437–1443.

Franklin, S. E., and Peddle, D. R. (1990), Classification of SPOT HRV imagery and texture features, *Int. J. Remote Sens.* 11:551–556.

Franklin, J. F., and Spies, T. A. (1991), Composition, function, and structure of old-growth Douglas-fir forests, in *Wildlife and Vegetation of Unmanaged Douglas-Fir Forests* (L. F. Ruggiero et al., Eds.), USDA Forest Service Gen. Tech. Rep. PNW-GTR-285, Portland, OR, pp. 71–80.

Franklin, J., and Strahler, A. H. (1988), Invertible canopy reflectance modeling of vegetation structure in semiarid woodland, *IEEE Trans. Geosci. Remote Sens.* GE-26:809–825.

Franklin, J., Logan, T. L., Woodcock, C. E., and Strahler, A. H. (1986), Coniferous forest classification and inventory using Landsat and digital terrain data, *IEEE Trans. Geosci. Remote Sens.* GE-24:139–149.

Franklin, J., Davis, F. W., and Lefebvre, P. (1991), Thematic Mapper analysis of tree cover in semiarid woodlands using a model of canopy shadowing, *Remote Sens. Environ.* 36: 189–202.

Gool, L. V., Dewaele, P., and Oosterlinck, A. (1985), Texture analysis anno 1983, *Comput. Vision Graph. Image Process.* 29:336–357.

Goward, S. N. (1990), Background spectral measurements for OTTER, unpublished memorandum, 24 June, Department of Geography, College Park, MD, 9 pp.

Guyot, G., Guyon, D., and Riom, J. (1989), Factors affecting the spectral response of forest canopies: a review, *Geocarto Int.* 4(3):3–18.

Holben, B., and Justice, C. (1980), The topographic effect on the spectral response of nadir-pointing sensors, *Photogramm. Eng. Remote Sens.* 46:1911.

Horler, D. N. H., and Ahern, F. J. (1986), Forestry information content of Thematic Mapper data, *Int. J. Remote Sens.* 7:405–428.

Irons, J. R., and Petersen, G. W. (1981), Textural transforms of remotely sensed data, *Remote Sens. Environ.* 11:359–370.

Iverson, L. R., Graham, R. L., and Cook, E. A. (1989), Applications of satellite remote sensing to forested ecosystems, *Landscape Ecol.* 3:131–143.

Johnson, G. R., Barthmaier, E. W., Gregg, T. W. D., and Aulds, R. E. (1979), Forest stand classification in western Washington using Landsat and computer-based resource data, in *Proceedings, Thirteenth International Symposium on Remote Sensing of Environment,* Ann Arbor, MI, 23–27 April 1979, ERIM, Ann Arbor, MI, pp. 1681–1696.

Justice, C. O., Wharton, S. W., and Holben, B. N. (1981), Application of digital terrain data to quantify and reduce the topographic effect on Landsat Data, *Int. J. Remote Sens.* 2:213–230.

Kimes, D. S., Newcomb, W. W., Nelson, R. F., and Schutt, J. B. (1986), Directional reflectance distributions of a hardwood and pine forest canopy, *IEEE Trans. Geosci. Remote Sens.* GE-24:281–293.

Li, X., and Strahler, A. H. (1985), Geometric-optical modeling of a conifer forest canopy, *IEEE Trans. Geosci. Remote Sens.* 23:705–721.

Mather, P. M. (1987), *Computer Processing of Remotely-Sensed Images,* Wiley, New York.

Musick, H. B., and Pelletier, R. E. (1988), Response to soil moisture of spectral indices derived from bidirectional reflectance in Thematic Mapper wavebands, *Remote Sens. Environ.* 25:167–184.

Niemann, K. O., Pilon, P. G., and Wairt, R. J. (1991), Generalized forest mapping using multi-temporal Landsat TM imagery: providing inputs into geographic information systems, in *Proceedings, 14th Canadian Symposium on Remote Sensing,* Calgary, Alberta, Canada, 6–10 May 1991, Canadian Remote Sensing Society, Ottawa, p. 142.

Peddle, D. R., and Franklin, S. E. (1991), Image texture processing and data integration for surface pattern discrimination, *Photogramm. Eng. Remote Sens.* 57:413–420.

Pouch, W., and Campagna, D. J. (1990), Hyperspherical direction cosine transformation for separation of spectral and illumination information in digital scanner data, *Photogramm. Eng. Remote Sens.* 56:475–479.

Proy, C., Tanré, D., and Deschamps, P. Y. (1989), Evaluation of topographic effects in remotely sensed data, *Remote Sens. Environ.* 30:21–32.

Rubin, T. (1990), Analysis of radar texture with variograms and other simplified descriptors, in *Proceedings, Image Processing '89,* Sparks, NV, 23 May 1989, ASPRS, Falls Church, VA, pp. 185–195.

Sabin, T. E., and Stafford, S. G. (1990), *Assessing the Need for Transformation of Response Variables,* Special Publ. 20, Forest Research Lab, College of Forestry, Oregon State University, 31 pp.

SAS (1991), *Statistical Analysis System,* version 6.03, SAS Institute, Cary, NC.

Smith, J. A., Lin, T. L., and Ranson, K. J. (1980), The Lambertian assumption and Landsat data, *Photogramm. Eng. Remote Sens.* 46:1183–1189.

Spanner, M. A., Pierce, L. L., Peterson, D. L., and Running, S. W. (1990), Remote sensing of temperate coniferous forest leaf area index: the influence of canopy closure, understory vegetation and background reflectance, *Int. J. Remote Sens.* 11:95–111.

Spies, T. A., and Cohen, W. B. (1991), An index of canopy height diversity, unpublished report, March 13, USDA Forest Service, Corvallis, OR, 5 pp.

Spies, T. A., and Franklin, J. F. (1991), The structure of natural young, mature, and old-growth forests in Washington and Oregon, in *Wildlife and Vegetaton of Unmanaged Douglas-Fir Forests* (L. F. Ruggiero et al., Eds.), USDA Forest Service Gen. Tech. Rep. PNW-GTR-285, Portland, OR, pp. 90–109.

Spies, T. A., Franklin, J. F., and Klopsch, M. (1990), Canopy gaps in Douglas-fir forests of the Cascade Mountains, *Can. J. For. Res.* 20:649–658.

Strahler, A. H. (1981), Stratification of natural vegetation for forest and rangeland inventory using Landsat digital imagery and collateral data, *Int. J. Remote Sens.* 2:15–41.

Teillet, P. M., Goodenough, D. G., Guindon, B., Meunier, J., and Dickinson, K. (1981), Digital analysis of spatial and spectral features from airborne MSS of a forested region, in *Proceedings, Fifteenth International Symposium on Remote Sensing of Environment,* Ann Arbor, MI, May 1981, ERIM, Ann Arbor, MI, pp. 883–903.

Teillet, P. M., Guindon, B., and Goodenough, D. G. (1982), On the slope-aspect correction of multispectral scanner data, *Can. J. Remote Sens.* 8:84–106.

Teply, J., and Green, K. (1991), Old growth forest, *Geo. Info. Syst.* 1(4):23–31.

Tom, C. H., and Miller, L. D. (1979), Forest site productivity mapping in the coniferous forests of Colorado with Landsat imagery and landscape variables, in *Proceedings, Thirteenth International Symposium on Remote Sensing of Environment,* Ann Arbor, MI, 23–27 April 1979, ERIM, Ann Arbor, MI, pp. 675–692.

Tucker, C. J. (1980), Remote sensing of leaf water content in the near infrared, *Remote Sens. Environ.* 10:23–32.

Walsh, S. J. (1980), Coniferous tree species mapping using LANDSAT data, *Remote Sens. Environ.* 9:11–26.

Walsh, S. J. (1987), Variability of Landsat MSS spectral responses of forests in relation to stand and site characteristics, *Int. J. Remote Sens.* 8:1289–1299.

Wang, L., and He, D. (1990), Texture classification using texture spectrum, *Pattern Recogn.* 23:905–910.

Wilderness Society (1991), *Ancient Forests in the Pacific Northwest,* The Wilderness Society, Washington, DC.

Woodcock, C. E., and Strahler, A. H. (1987), The factor of scale in remote sensing, *Remote Sens. Environ.* 21:311–332.

Woodcock, C. E., Harward, V. J., Jakabhazy, V., et al. (1990), An overview of a new timber inventory system, in *Proceedings of the Third Forest Service Remote Sensing Applications Conference,* Tucson, AZ, 9–13 April, 1990, ASPRS, Bethesda, MD, pp. 321–333.